Aminopropyltriethoxysilane (APTES)-functionalized nanoporous polymeric gratings: fabrication and application in biosensing

Vincent K. S. Hsiao,[a] John R. Waldeisen,[a] Yuebing Zheng,[a] Pamela F. Lloyd,[b] Timothy J. Bunning[b] and Tony Jun Huang*[a]

Received 23rd July 2007, Accepted 28th September 2007
First published as an Advance Article on the web 12th October 2007
DOI: 10.1039/b711200a

We have fabricated aminopropyltriethoxysilane (APTES)-functionalized nanoporous polymeric gratings by combining holographic interference patterning and APTES-functionalization of the pre-polymer syrup. The APTES facilitates the immobilization of biomolecules onto the polymeric grating surfaces. The successful detection of multiple biomolecules (biotin, steptavidin, biotinylated anti-rabbit IgG, and rabbit-IgG) indicates that the functionalized nanoporous polymeric gratings can act as biosensing platforms which are label-free, inexpensive, and applicable as high-throughput assays.

Introduction

The sensing and monitoring of biological molecules such as proteins, enzymes, and DNA are of tremendous importance in applications such as gene mapping,[1] clinical diagnostics,[2] and drug discovery.[3] Ideal biosensing methods have to be sensitive, selective, rapid, cost-effective, and label-free.[4] Specifically, a label-free biosensor eliminates the need for tedious fluorescence or radioactive labeling processes,[5] while providing rapid and convenient signal transduction by converting the molecular-recognition events into electrochemical,[6] optical,[7] acoustic,[8] or calorimetric[9] signals. Porous silicon has been demonstrated as an appealing platform for label-free optical detection as the large internal surface area facilitates high-throughput and sensitive biosensing.[10] Various analytes, such as DNA,[11] protein,[12] enzymes,[13] pathogens,[14] and bacteria,[15] have been detected with porous silicon-based biosensors using different immobilization protocols.

The authors have developed a method for creating periodic nanopores encased within polymer matrices by modifying the traditional holographic, polymer-dispersed liquid crystal (H-PDLC) system.[16] This technique entails holographic interference patterning upon a modified photopolymer mixed with a non-reactive solvent, making possible the rapid fabrication of nanoporous polymeric gratings of varying dimensions. The successful demonstration of reflective optical elements with large internal surface areas as organic vapor sensors[17] reveals the structures' potential for use as a platform for high-throughput sensing. However, application of the gratings for biosensing has been hindered due to the inability of the as-prepared polymers to immobilize biomolecules. To enhance the immobilization of biomolecules on polymeric gratings, functionalizing each polymeric grating with molecules that can serve as an interface between the grating and biomolecules is one of the most straightforward and efficient solutions.

Aminopropyltriethoxysilane (APTES) has been widely used in affinity-based biosensors because the silane group can tightly bind to silicon or glass substrates, while its amine group can form covalent bonds with carboxyl groups (functional groups that are commonly found in biomolecules).[18] In this paper, we develop the technique to produce APTES-functionalized nanoporous polymer gratings for biosensing. The high index modulation (0.07) of the gratings is generated by nanopores that provide a high signal-to-noise ratio. The direct addition of APTES into the photopolymer syrup effectively facilitates the capture of biomolecules, such as biotin, onto the nanoporous region. The binding between biomolecules and functionalized nanopores is detectable by simply observing the optical modulation in the grating efficiency. A series of sensing experiments with multiple biomolecules reveals the capability of functionalized gratings to perform as biosensing platforms.

Experimental

Fabrication of nanoporous polymeric gratings

The final composition of the photopolymer syrup contained 10 wt% APTES (Aldrich), 25 wt% acetone solution (Aldrich), 15 wt% TL213 liquid crystal (Merck), 40 wt% dipentaerythritol hydroxypentaacrylate (Aldrich), 1 wt% Rose Bengal (Spectra Group Limited), 2 wt% *N*-phenylglycine (Aldrich), and 7 wt% *N*-vinylpyrrolidinone (Aldrich). To fabricate the APTES-functionalized, nanoporous polymeric structures, APTES was first mixed homogeneously into the photopolymer syrup with a mixer and a sonicator (VWR). Second, 20 μL of syrup was added onto a glass slide and covered with a second glass slide coated with a non-reactive 100 nm gold layer. Third, a 514 nm argon ion laser was used to conduct holographic interferometry. In this step, the sandwiched sample was exposed to two 100 mW laser beams at a writing angle of 30° for one minute. Fourth, immediately following the interference patterning, the sandwiched sample was post-cured under a white light source for 24 h. Upon separating

[a]*Department of Engineering Science and Mechanics, The Pennsylvania State University, 212 Earth Engineering Science Building, University Park, PA, 16802, USA. E-mail: junhuang@psu.edu*
[b]*Air Force Research Laboratory, Materials and Manufacturing Directorate Wright-Patterson Air Force Base, Dayton, OH, 45433, USA*

the sample from the cover slide, an APTES-functionalized nanoporous polymer grating structure situated on a glass slide was obtained.

Analysis of chemical composition

The chemical composition of APTES-functionalized gratings was analyzed by Fourier-transform infrared (FT-IR) spectroscopy. All the transmission spectra were acquired using a Nicolet 6700 FT-IR spectrometer (Thermo Electron Corporation, Waltham, MA) and a liquid nitrogen-cooled, mercury cadmium telluride detector. The spectrometer setup was purged with dry, CO_2-free air delivered from a purge gas generator (Parker-Balston, Cleveland, OH). All IR data were measured in transmission mode with a mirror speed of 1.8988 cm s^{-1} and a resolution of 2 cm^{-1} averaged over 32 scans. A plain glass slide was used as a reference.

Morphology analysis

The morphology of the samples was investigated using low-voltage SEM (Hitachi S-900) and bright-field TEM (Jeol 100CX). The sample preparation was as follows: the cross-sections of the films were prepared by fracturing the sample in liquid N_2 and mounting the sample on its edge in conductive silver paint. SEM was operated at 1 keV, while TEM was operated at 100 keV. The samples for TEM were prepared by ultramicrotomy at room temperature from epoxy blocks. As a result, the bright regions of the images show air voids filled by the epoxy while the grey regions show the polymer.

Biotin immobilization and optical data acquisition

The biotin solution was prepared by dissolving sulfo-NHS-LC-LC-biotin (G-Bioscience) in phosphate-buffered saline (PBS) and diluting to desired concentrations. For each sample, the polymer grating was immersed and incubated in the desired concentration of biotin solution for one hour. Next, the sample was rinsed by complete immersion in PBS for five minutes and dried by applying a direct air flow to the substrate. The sample was then subjected to optical measurement performed with a collimated He–Ne laser (632.8 nm, 5 mW, 500 : 1, Thorlabs) at an incident angle of 30°. Two silicon photodetectors (DET series, Thorlabs) recorded the intensity of first-order diffracted and transmitted light. Both diffraction efficiency and transmission efficiency were normalized without considering scattering effects from the grating film. A photodiode amplifier (PDA-700, Terahertz Technologies) amplified the signals from the photodetectors and transferred the input photocurrent into a recordable output voltage.

Results and discussion

Fig. 1 depicts the surface and cross-sectional morphology of a nanoporous polymeric grating before APTES functionalization, as characterized by low-voltage scanning electron microscopy (SEM) and bright-field transmission electron microscopy (TEM). The grating is comprised of cross-linking polymer areas (non-porous regions) and periodically alternating nanoporous polymer areas (porous regions) consisting of nanopores and granular polymer. The size of the nanopores

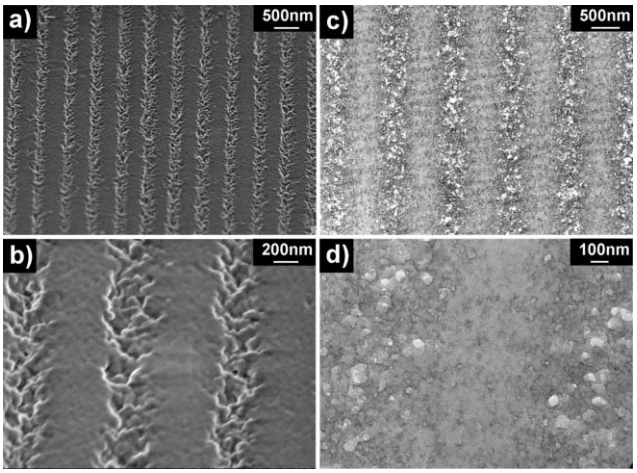

Fig. 1 Morphology of nanoporous polymer gratings: a) and b) are the surface morphology characterized by SEM; c) and d) are the cross-sectional morphology characterized by TEM. Bright regions on the TEM images are air voids.

ranges from 20 nm to 100 nm. The periodicity of the polymeric gratings is measured to be ~650 nm, which is in good agreement with calculated results (~670 nm) from the Bragg diffraction equation.[19]

To fabricate the APTES-functionalized nanoporous polymeric gratings, APTES is directly mixed into the photopolymer syrup followed by holographic interference patterning. Fig. 2 shows the result of FT-IR spectroscopic analysis upon the fabricated grating samples without (curve a) and with (curve b) the functionalization of APTES. The FT-IR spectrum of the APTES-functionalized sample showed new peaks at 3300 cm^{-1} (indicating the NH_2 stretch vibration) and 2972 cm^{-1} (indicating the –C–NH_2 stretch vibration). On the other hand, the peak at 2954 cm^{-1} (indicating the C–H stretch) that was observed in the non-APTES grating sample disappeared in the APTES-functionalized sample. The FT-IR results prove that mixing APTES into the photopolymer syrup is an efficient way to functionalize the polymeric nanostructure.

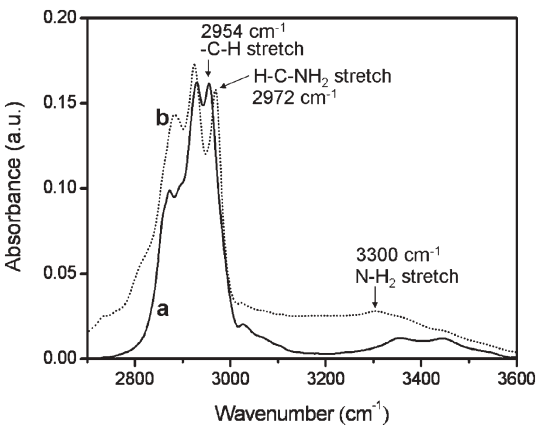

Fig. 2 FT-IR spectra of nanoporous polymer gratings: a) without the addition of APTES; b) with the addition of 30 wt% APTES into the photopolymer before holographic interferometry.

The addition of a high concentration of APTES stabilizes the polymer film and binds biomolecules onto the nanoporous surface. However, excessive APTES decreases the grating's diffraction efficiency, a key parameter for the sensitivity of a diffraction-based biosensor.[20] Fig. 3(a) shows that the grating sample's diffraction efficiency decreases as the amount of APTES increases. We adjusted the APTES concentration in the pre-polymer syrup so that it was high enough to guarantee biomolecular binding onto the nanoporous surface, but low enough to not affect the formation of nanopores and periodic structures during the holographic fabrication process. Fig. 3(b) and (c) show the FT-IR spectra of the APTES-functionalized samples at different APTES concentrations. The characteristic peaks (2972 cm^{-1} and 3300 cm^{-1}) attributed to the amine groups were observed only when the samples contained more than or equal to 10 wt% APTES. This concentration was chosen for the nanoporous polymer grating-based biosensors, because it offers sufficient amine groups for biomolecular binding to the surface, while maintaining high grating efficiency ($\sim$80%).

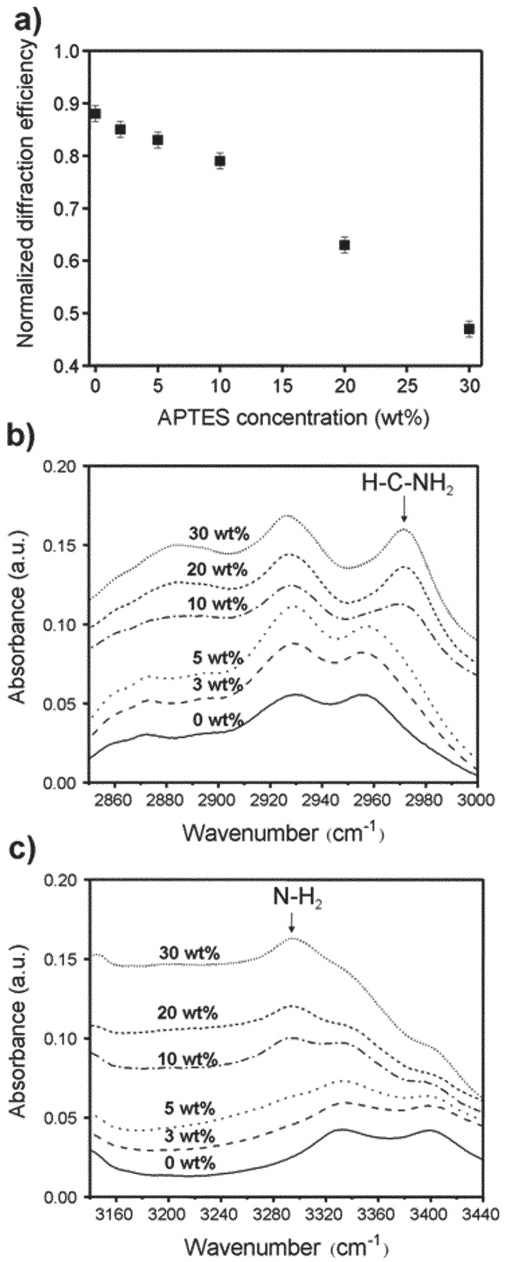

Fig. 3 (a) Dependence of diffraction efficiency of a nanoporous polymer grating structure on the APTES concentration. Evolution of b) $-C-NH_2$ peak and c) amine peak in FT-IR spectra from nanoporous polymer gratings containing different weight percentages of APTES added into the photopolymer.

In diffraction-based biosensors,[20] the refractive index (RI) modulation can be taken as an indicator for the immobilization of analytes onto the transducers. High index modulation of a nanoporous grating structure depends highly on the nanoporous region as this region enables the observation of changes in the grating's transmission efficiency while enhancing the signal-to-noise ratio. Therefore it is essential to characterize the performance of the bioassay through quantitative analysis of the nanoporous polymer gratings' index modulation. According to the Kogelnik coupled wave theory,[21] the grating's diffraction efficiency (η) for a lossless dielectric diffraction element can be expressed as:

$$\eta = \sin^2(v^2 + \varepsilon^2)^{1/2}/(1 + \varepsilon^2/v^2) \quad (1)$$

where v and ε are determined by the following equations:

$$v = \pi\Delta n d/\lambda\cos\theta \quad (2)$$

$$\varepsilon = n_{ave}\pi d(\theta - \theta_{Bragg})\sin(2\theta_{Bragg})/\lambda\cos\theta \quad (3)$$

In eqn (2) and (3), d is the grating thickness; n_{ave} is the average refractive index; Δn is the refractive index modulation; λ is the writing wavelength for holographic interferometry; θ is the incident angle of the sample; and $\Delta\theta$ is the deviation from the Bragg angle θ_{Bragg}. Diffraction experiments (Fig. 4) were conducted to calculate the grating structure's index modulation, which was found by fitting the experimental data of incident angle (θ) *vs.* diffraction efficiency (η) to eqn (1).[22] Δn was found to be 0.07. To our knowledge, the index modulation achieved in this report is among the highest of all holographic polymer grating structures reported in the literature.[23]

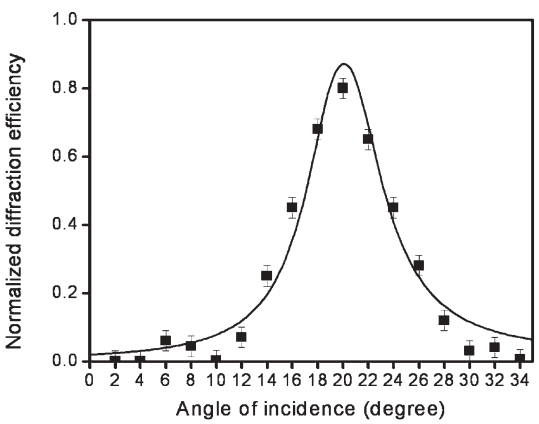

Fig. 4 Nanoporous polymer grating's diffraction efficiency dependence on the incident angle of monochromatic light from a 632 nm He–Ne laser. Experimental data are depicted by solid squares; theoretical simulation is represented by a solid line.

The APTES-functionalized nanoporous polymer gratings with high RI modulation demonstrated here are excellent platforms for label-free biosensing. The grating's sensory capability is based on changes of RI before and after immobilization of analytes between the porous and nonporous regions. For example, when biotin (RI = 1.43) binds onto the nanopores (RI = 1), the index modulation on the grating is reduced along with its diffraction efficiency, according to eqn (1). Based on the diffraction theory, the Bragg angle of the observed light can be fixed and the nanoporous polymer grating's diffraction and transmission responses to biomolecules can be monitored, thereby establishing the nanoporous polymer grating's effectiveness as a biosensor. Fig. 5 shows the optical response of the grating at different biotin concentrations. The diffraction efficiency decreases (Fig. 5a) and the transmission efficiency increases (Fig. 5b), with a corresponding increase in biotin concentration. The diffraction efficiency shows a linear decrease from $\sim$80% to $\sim$70% when biotin concentration increases from 0 to 0.5 mg mL^{-1} before it deviates from linearity at higher biotin concentrations (1 mg mL^{-1}). The dependence of the grating's diffraction efficiency on biomolecular concentration is consistent with the proposed mechanism that the nanoporous grating is sensitive to RI variations caused by biomolecular immobilization, indicating the method's potential for quantitative biosensing.

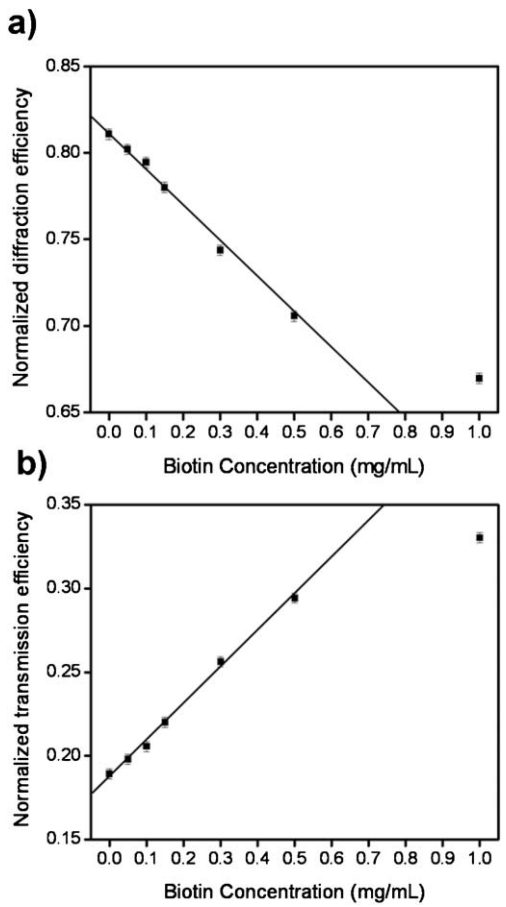

Fig. 5 Dependence of a) diffraction and b) transmission efficiency on biotin concentration.

In a control study, we immersed a nanoporous polymer grating into a pure PBS solution for periods of time and observed either no change in diffraction and transmission efficiencies or a slight decrease in both efficiencies. The latter case is attributed to light scattering from the polymer surfaces after immersion in PBS. However, the decrease of both the diffraction efficiency and transmission efficiency is trivial. A grating held in PBS solution for more than twenty-four hours retained more than 90% of its diffraction and transmission signals, indicating that aqueous environments do not inhibit the films' ability to monitor changes. Based on the diffraction/transmission study of biotin attachment and the control study of immersing the sample in PBS buffer, we can conclude that the decrease in diffraction efficiency and the corresponding increase in transmission suggest effective immobilization of biomolecules.

The immobilization of biotin onto the nanoporous regions can be directly observed from the sample morphology. Fig. 6 shows two TEM micrographs of the biotin-functionalized grating. The binding of biotin to the nanoporous regions is indicated by the dark outline surrounding the pores; the dark outline is not observed in samples without biotin functionalization (Fig. 1(c) and (d)). The biotin binding reduces the size of the voids, increases the average index of the nanoporous regions, and decreases the grating's diffraction efficiency, as observed from Fig. 5.

The optical and morphological observations not only show that mixing APTES into the pre-polymer syrup enables biotin immobilization on the nanoporous areas, but also proves that the optical response induced by biomolecular attachment is strong enough to be detected. Our next goal was to establish that the nanoporous, polymer grating-based biosensor could be extended to the detection of larger biomolecules and more complicated biological interactions, such as antibody/protein binding. The detection of rabbit IgG, a biomarker commonly used to detect infectious diseases,[24] was investigated through a multi-step bioassay. Fig. 7(a) illustrates the sequence of biomolecular interactions that occur within the nanopores in preparation for the antibody/antigen assay. The APTES-functionalized grating was first immobilized with biotin. Streptavidin was then selectively captured onto the biotin-functionalized nanoporous areas. Upon exposure of biotinylated anti-rabbit IgG to the sensor surface, it was immobilized on the surface by a second biotin–streptavidin interaction. The anti-rabbit IgG then selectively captured and detected rabbit IgG.

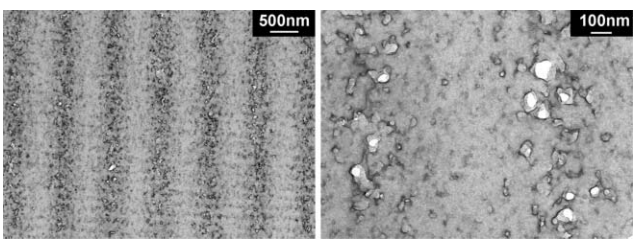

Fig. 6 TEM characterization of the cross-sectional morphology of a nanoporous polymer grating after the grating was incubated with biotin. The dark outlines indicate the biotin binding to the nanoporous surface.

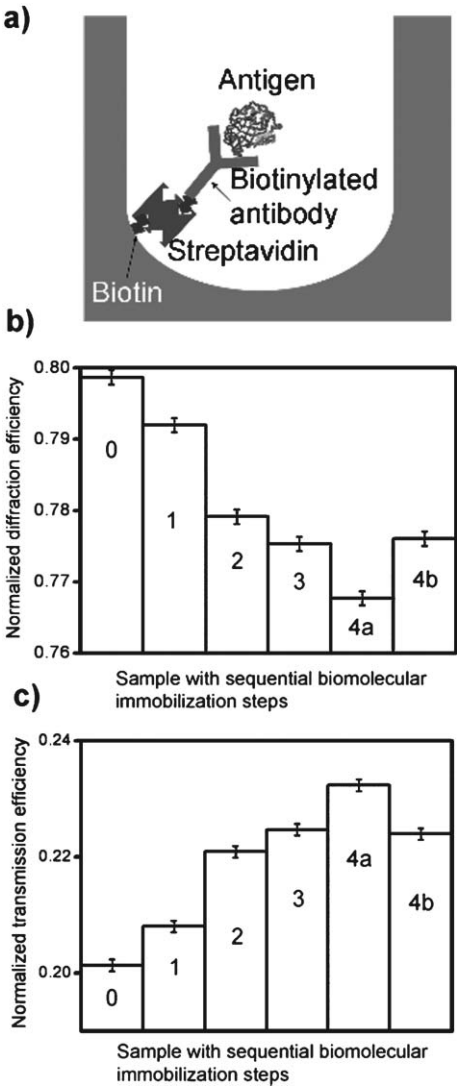

Fig. 7 (a) A schematic of the biodetection assay; (b) and (c) are the observed changes in diffraction and transmission efficiencies, respectively, with sequential surface immobilization steps. Step 0: original sample; step 1: sample incubated in 50 μg mL^{-1} biotin solution; step 2: sample incubated in 50 μg mL^{-1} streptavidin solution; step 3: sample incubated in 20 μg mL^{-1} biotinylated anti-rabbit IgG solution; step 4a: sample incubated in 20 μg mL^{-1} rabbit IgG solution; step 4b: sample incubated in 20 μg mL^{-1} goat IgG solution.

Fig. 7(b) and (c) show that the diffraction efficiency decreases and the corresponding transmission efficiency increases sequentially when the grating is incubated with biotin (step 1), streptavidin (step 2), biotinylated anti-rabbit IgG (step 3), and rabbit IgG (step 4a) solutions. In the control experiment (step 4b), step 4a was replaced with the incubation of goat IgG (control molecule), and the diffracted light intensity decrease was much smaller. In addition, instead of detecting a transmitted intensity increase as in step 4a, we observed that the transmitted light intensity slightly decreased with the control protein. This observation indicates non-effective immobilization, which was also observed in the previously mentioned control experiment involving pure PBS buffer as the detection target. Our experimental data indicate that the non-specific binding between goat IgG and anti-rabbit IgG was negligible, and that the assay was highly specific.

The subsequent immobilization of biotin and streptavidin (steps 1 and 2 in Fig. 7) was essential to the immobilization of biotinylated anti-rabbit IgG onto the nanoporous polymer surface. The decrease of diffraction efficiency and increase of transmission efficiency were not observed upon direct exposure of the APTES-functionalized nanoporous polymer to streptavidin or biotinylated anti-rabbit IgG solution. In addition, we found that relatively low concentrations of biotin and streptavidin were necessary for further immobilization of antibodies and antigens upon the void interface. Higher concentrations (>100 μg mL^{-1}) of biotin and streptavidin resulted in the saturation of these two analytes on the nanoporous areas, preventing subsequent immobilization steps.

Conclusions

We have developed the ATPES-functionalized nanoporous polymeric gratings for use as biosensing platforms. Experimental results showed that mixing APTES into the photopolymer before holographic interferometry is an effective way to generate APTES-functionalized polymer structures that facilitate the immobilization of biomolecules. The resulting APTES-functionalized gratings possess a high RI modulation of 0.07, a characteristic crucial in optical biosensing applications. The gratings also prove effective in detecting various biological substances, from small biotin to much larger rabbit IgG molecules. The fabrication and biosensing method described here is inexpensive, safe, and label-free. Moreover, the large surface area of these nanoporous polymeric structures makes them suitable for high-throughput applications.

Acknowledgements

This work was supported in part by the Grace Woodward Grants for Collaborative Research in Engineering and Medicine, the NSF NIRT grant (ECCS-0609128), and the start-up fund provided by the Engineering Science and Mechanics Department, College of Engineering, Materials Research Institute, and Huck Institutes for the Life Sciences at The Pennsylvania State University. The authors thank Hector M. Saavedra for help with FT-IR measurement, and Thomas R. Walker, Ji Lee, Nicholas Fang, and Paul Bonvallet for their helpful discussion.

References

1 (*a*) R. W. Davis and P. O. Brown, *Science*, 1995, **270**, 467; (*b*) M. Kitamura, A. Kasai, Y. Meng, N. Hiramatsu and J. Yao, *Biophys. & Biochem.*, 2004, **4**, 243.
2 C. Mueller, B. Hitzmann, F. Schubert and T. Scheper, *Sens. Actuators, B*, 1997, **40**, 71.
3 (*a*) P. R. Coulet, L. J. Blum and S. M. Gautier, *J. Pharm. Biomed. Anal.*, 1989, **7**, 1361; (*b*) M. Minunni, S. ombelli, M. Mascini, A. Bilia, M. C. Bergonzi and A. F. F. Vincieri, *Talanta*, 2005, **65**, 578; (*c*) S. A. Haughey and G. A. Baxter, *J. AOAC Int.*, 2006, **89**, 862.
4 (*a*) P. Vadgama and P. W. Crump, *Analyst*, 1992, **117**, 1657; (*b*) A. P. F. Turner, *Science*, 2000, **290**, 1315; (*c*) M. A. Cooper, *Nat. Rev. Drug Discovery*, 2002, **1**, 515; (*d*) T. Vo-Dinh and L. Allain, *Biomedical Photonics: Handbook*, CRC Press,Boca Raton, 2003.

5 (*a*) J. D. Brennan, *J. Fluoresc.*, 1999, **9**, 295; (*b*) S. Y. Rabbany, W. J. Lane, W. A. Marganski, A. W. Kusterbeck and F. S. Ligler, *J. Immunol. Methods*, 2000, **246**, 69; (*c*) S. Ekgasit, G. Stengel and W. Knoll, *Anal. Chem.*, 2004, **76**, 4747; (*d*) K. S. Ko, F. A. Jaipuri and N. L. Pohl, *J. Am. Chem. Soc.*, 2005, **127**, 13162; (*e*) E. S. Barker, J. W. Hong, B. S. Gaylord, G. C. Bazan and M. T. Bowers, *J. Am. Chem. Soc.*, 2006, **128**, 8484.

6 (*a*) J. Wang, G. Rivas, X. Cai, E. Palecek, P. Nielsen, H. Shiraishi, N. Dontha, D. Luo, C. Parrado, M. Chicharro, P. A. M. Farias, F. S. Valera, D. H. Grant, M. Ozsoz and M. N. Flair, *Anal. Chim. Acta*, 1997, **347**, 1; (*b*) B. K. Jena and C. R. Raj, *Anal. Chem.*, 2006, **78**, 6332; (*c*) J. A. Hansen, J. Wang, A. Kawde, Y. Xiang, K. V. Gothelf and G. Collins, *J. Am. Chem. Soc.*, 2006, **128**, 2228; (*d*) T. Huang, M. Liu, L. D. Knight, W. W. Grody, J. F. Miller and C. M. Ho, *Nucleic Acids Res.*, 2002, **30**, e55.

7 (*a*) Y. G. Tsay, C. I. Lin, J. Lee, E. K. Gustafson, R. Appelqvist, P. Magginetti, R. Norton, N. Teng and D. Charlton, *Clin. Chem.*, 1991, **37**, 1502; (*b*) P. M. John, R. Davis, R. Cady, J. Czajka, C. A. Batt and H. G. Craighead, *Anal. Chem.*, 1998, **70**, 1108; (*c*) J. B. Goh, R. W. Loo, R. A. McAloney and M. C. Goh, *Anal. Bioanal. Chem.*, 2002, **374**, 54; (*d*) A. J. Haes and R. P. Van Duyne, *J. Am. Chem. Soc.*, 2002, **124**, 10596; (*e*) S. Pan and L. J. Rothberg, *Nano Lett.*, 2003, **3**, 811; (*f*) R. C. Bailey, J. Nam, C. A. Mirkin and J. T. Hupp, *J. Am. Chem. Soc.*, 2003, **125**, 13541; (*g*) P. T. Fiori and M. F. Paige, *Anal. Bioanal. Chem.*, 2004, **380**, 339; (*h*) K. Mitsui, Y. Handa and K. Kajikawa, *Appl. Phys. Lett.*, 2004, **85**, 4231; (*i*) B. Yuan, Y. Hao and Z. Tan, *Clin. Chem.*, 2004, **50**, 1057; (*j*) A. J. Haes, L. Chang, W. L. Klein and R. P. Van Duyne, *J. Am. Chem. Soc.*, 2005, **127**, 2264; (*k*) X. Wang and U. J. Krull, *J. Mater. Chem.*, 2005, **15**, 2801.

8 (*a*) K. Bonroy, J. Friedt, F. Frederix, W. Laureyn, S. Langerock, A. Campitell, M. Sara, G. Borghs, B. Goddeeris and P. Declerck, *Anal. Chem.*, 2004, **76**, 4299; (*b*) A. C. Stevenson, B. Araya-Kleinsteuber, R. S. Sethi, H. M. Mehta and R. C. Lowe, *J. Mol. Recognit.*, 2004, **17**, 174; (*c*) A. Zhou and J. Muthuswamy, *Sens. Actuators, B*, 2004, **101**, 8.

9 (*a*) H. G. Hundeck, M. Weiss, T. Scheper and F. Schubert, *Biosens. Bioelectron.*, 1993, **8**, 205; (*b*) M. Kolb and B. Zentgraf, *J. Chem. Technol. Biotechnol.*, 1996, **66**, 15.

10 (*a*) V. S. Y. Lin, K. Motesharei, K. S. Dancil, M. J. Sailor and M. R. Ghadiri, *Science*, 1997, **278**, 840; (*b*) S. Chan, Y. Li, L. J. Rothberg, B. L. Miller and P. M. Fauchet, *Mater. Sci. Eng., C*, 2001, **15**, 277; (*c*) S. Huh, J. W. Wiench, J.-C. Yoo, M. Pruski and V. S. Y. Lin, *Chem. Mater.*, 2003, **15**, 4247; (*d*) L. A. DeLouise, P. M. Fauchet, B. L. Miller and A. A. Pentland, *Adv. Mater.*, 2005, **17**, 2199; (*e*) V. Torres-Costa, F. Agullo-Rueda, R. J. Martin-Palma and J. M. Martinez-Duart, *Opt. Mater.*, 2005, **27**, 1084; (*f*) L. De Stefano, L. Rotiroti, I. Rendina, L. Moretti, V. Scognamiglio, M. Rossi and S. D'Auria, *Biosens. Bioelectron.*, 2006, **21**, 1664–1667; (*g*) M. H. Klühr, A. Sauermann, C. A. Elsner, K. H. Thein and S. K. Dertinger, *Adv. Mater.*, 2006, **18**, 3135; (*h*) I. I. Slowing, B. G. Trewyn, S. Giri and V. S.-Y. Lin, *Adv. Funct. Mater.*, 2007, **17**, 1225.

11 (*a*) T. Vo-Dinh, J. P. Alarie, N. Isola, D. Landis, A. L. Wintenberg and M. N. Ericson, *Anal. Chem.*, 1999, **71**, 358; (*b*) M. Archer, M. Christophersen and P. M. Fauchet, *Biomed. Microdev.*, 2004, **6**, 203; (*c*) G. Di Francia, V. La Ferrara, S. Manzo and S. Chiavarini, *Biosens. Bioelectron.*, 2005, **21**, 661; (*d*) M. J. Kim, M. Wanunu, D. C. Bell and A. Meller, *Adv. Mater.*, 2006, **18**, 3149.

12 (*a*) K. S. Dancil, D. P. Greiner and M. J. Sailor, *J. Am. Chem. Soc.*, 1999, **121**, 7925; (*b*) M. M. Orosco, C. Pacholski, G. M. Miskelly and M. J. Sailor, *Adv. Mater.*, 2006, **18**, 1393; (*c*) H. Ouyang, C. C. Striemer and P. M. Fauchet, *Appl. Phys. Lett.*, 2006, **88**, 163108–1; (*d*) F. Vollmer, D. Braun, A. Libchaber, M. Khoshsima, I. Teraoka and S. Arnold, *Appl. Phys. Lett.*, 2002, **80**, 4057.

13 (*a*) T. Laurell, J. Drott, L. Rosengren and K. Lindstroem, *Sens. Actuators, B*, 1996, **31**, 161; (*b*) S. E. Letant, B. R. Hart, S. R. Kane, M. Z. Hadi, S. J. Shields and J. G. Reynolds, *Adv. Mater.*, 2004, **16**, 689; (*c*) S. Sotiropoulou, V. Vamvakaki and N. A. Chaniotakis, *Biosens. Bioelectron.*, 2005, **20**, 1674; (*d*) W. H. Scouten, J. H. t. Luong, R. S. Brown, L. A. DeLouise, P. M. Kou and B. L. Miller, *Anal. Chem.*, 2005, **77**, 3222.

14 F. P. Mathew and E. C. Alocilja, *Biosens. Bioelectron.*, 2005, **20**, 1656.

15 S. Chan, S. R. Horner, P. M. Fauchet and B. L. Miller, *J. Am. Chem. Soc.*, 2001, **123**, 11797.

16 (*a*) V. K. S. Hsiao, T. C. Lin, G. S. He, A. N. Cartwright, P. N. Prasad, L. V. Natarajan, V. P. Tondiglia and T. J. Bunning, *Appl. Phys. Lett.*, 2005, **86**, 131113–1; (*b*) K. R. Maskaly, V. K. S. Hsiao, A. N. Cartwright, P. N. Prasad, P. F. Lloyd, T. J. Bunning and W. C. Carter, *J. Appl. Phys.*, 2006, **100**, 066103–1.

17 V. K. S. Hsiao, W. D. Kirkey, F. Chen, A. N. Cartwright, P. N. Prasad and T. J. Bunning, *Adv. Mater.*, 2005, **17**, 2211.

18 T. Cass and F. S. Ligler, *Immobilized biomolecules in analysis: A practical approach*, Oxford University Press, New York, 1998.

19 T. J. Bunning, L. V. Natarajan, V. P. Tondiglia and R. L. Sutherland, *Annu. Rev. Mater. Sci.*, 2000, **30**, 83.

20 (*a*) H. L. Wald, G. Sarakinos, M. D. Lyman, A. G. Mikos, J. P. Vacanti and R. Langer, *Biomaterials*, 1993, **14**, 270; (*b*) T. A. Desai, D. J. Hansford, L. Kulinsky, A. H. Nashat, G. Rasi, J. Tu, Y. Wang, M. Zhang and M. Ferrari, *Biomed. Microdev.*, 1999, **2**, 11; (*c*) O. A. Saleh and L. L. Sohn, *Nano Lett.*, 2003, **3**, 37; (*d*) W. Qian, Z. Gu, A. Fujishima and O. Sato, *Langmuir*, 2002, **18**, 4526; (*e*) A. Valsesia, P. Colpo, M. Manso Silvan, T. Meziani, G. Ceccone and F. Rossi, *Nano Lett.*, 2004, **4**, 1047; (*f*) H. C. Kim, G. Wallraff, C. R. Kreller, S. Angelos, V. Y. Lee, W. Volksen and R. D. Miller, *Nano Lett.*, 2004, **4**, 1169.

21 H. Kogelnik, *Bell Sys. Tech. J.*, 1969, **48**, 2909.

22 The thickness of the film d = 3.0 μm, the writing wavelength λ of 514 nm, and Bragg angle θ_{Bragg} of 30° were obtained experimentally. The RI of the nanoporous polymer films was calculated based on the experimental results on the RI of polymer syrup (1.51, from direct measurement) and porosity (10%, from SEM and TEM results).

23 (*a*) M. Jazbinsek, O. Drevensek, Z. Irena, F. Marko, K. Adam and G. P. Crawford, *J. Appl. Phys.*, 2001, **90**, 3831; (*b*) T. J. Trout, J. J. Schmieg, W. J. Gambogi and A. M. Weber, *Adv. Mater.*, 1998, **10**, 1219; (*c*) S. Massenot, J. Kaiser, R. Chevallier and Y. Renotte, *Appl. Opt.*, 2004, **43**, 5489; (*d*) Y. J. Liu, X. W. Sun, P. Shum, H. P. Li, J. Mi, W. Ji and X. H. Zhang, *Appl. Phys. Lett.*, 2006, **88**, 061107–1.

24 J. Gutierrez and C. Maroto, *Microbios*, 1996, **87**, 113.